International Journal of Earth, Energy and Environmental Sciences
ISSN: 2517-942X
Vol:8, No:5, 2014

Estimation of Seismic Ground Motion and Shaking Parameters Based On Microtremor Measurements at Palu City, Central Sulawesi Province, Indonesia

P. S. Thein, S. Pramumijoyo, K. S. Brotopuspito, J. Kiyono, W. Wilopo, A. Furukawa, A. Setianto

***Abstract*—**In this study, we estimated the seismic ground motion parameters based on microtremor measurements at Palu City. Several earthquakes have struck along the Palu-Koro Fault during recent years. The USGS epicenter, magnitude Mw 6.3 event that occurred on January 23, 2005 caused several casualties. We conducted a microtremor survey to estimate the strong ground motion distribution during the earthquake. From this survey we produced a map of the peak ground acceleration, velocity, seismic vulnerability index and ground shear strain maps in Palu City. We performed single observations of microtremor at 151 sites in Palu City. We also conducted 8-site microtremors array investigation to gain a representative determination of the soil condition of subsurface structures in Palu City. From the array observations, Palu City corresponds to relatively soil condition with Vs ≤ 300 m/s, the predominant periods due to horizontal vertical ratios (HVSRs) are in the range of 0.4 to 1.8 s and the frequency are in the range of 0.7 to 3.3 Hz. Strong ground motions of the Palu area were predicted based on the empirical stochastic green's function method. Peak ground acceleration and velocity becomes more than 400 gal and 30 kine in some areas, which causes severe damage for buildings in high probability. Microtremor survey results showed that in hilly areas had low seismic vulnerability index and ground shear strain, whereas in coastal alluvium was composed of material having a high seismic vulnerability and ground shear strain indication.

***Keywords*—**Palu-Koro Fault, Microtremor, Peak Ground Acceleration, Peak Ground Velocity and Seismic Vulnerability Index.

I. Introduction

PALU City is provincial capital of Sulawesi Tengah that it was divided into 4 districts and 43 villages. Palu City had an area of 395, 06 square kilometer and densely populated with more than 335, 297 people, that is located at the Palu bay and Palu valley plain area, in accordance to astronomicis located between 0º, 46' - 0º, 60' south latitude and 119º, 49' - 119°, 57' east longitude, it is appropriately under the equator with height 0 to 700m from surface of the sea (Fig. 1).

Pyi Soe Thein, Subagyo Pramumijoyo, Wahyu Wilopo, and Agung Setianto are with the Geological Engineering Department, Gadjah Mada University, Yogyakarta, Indonesia (phone: 628-121-523-3960; e-mail: pyisoethein@yahoo.com, bagyo@ugm.ac.id, wwilopo@gadjahmada.edu, agung.setianto@gmail.com).

Kirbani Sri Brotopuspito is with the Physics Department, Gadjah Mada University, Yogyakarta, Indonesia (e-mail: kirbani@yahoo.com).

Junji Kiyono and Aiko Furukawa are with the Graduate School of Global Environmental Studies, Kyoto University, Japan (e-mail: kiyono.junji.5x@kyoto-u.ac.jp, furukawa.aiko.3w@kyoto-u.ac.jp).

Fig. 1 Location map of Palu City [1]

II. Seismicity

Based on USGS catalog [2] more than hundred earthquakes with magnitude more than 7 were recorded in Sulawesi area. These earthquakes clustered at the northern arm of Sulawesi and along the Palu-Koro Fault System.

December 1, 1927 earthquake: This earthquake originated at -0.7 S° and 119.7 E° with the magnitude of 6.3. It shocked West Central Sulawesi, Palu City area, resulted in 15m height tsunami occurred, 14 killed, 30 injured and 0.5 to 12 m subsidence.

March 7, 1960 earthquake: It occurred at -1.5000 N° and 125.5000 E° with moderate intensities in regional scale with the magnitude of 5.1 and the depth of 60 km.

April 11, 1967 earthquake: This earthquake occurred at -3.3 S° and 119.4 E° with the magnitude of 6.3 and thrust fault mechanism. Tinambung area felt maximum intensity of VIII – VIII, resulted in 58 killed, 100 injured and the water suddenly retreated.

August 14, 1968 earthquake: It originated at -0.7 N° and 118.8 E° with high intensities magnitude of 7.4 and normal fault mechanism. West Central Sulawesi, Palu bay felt maximum intensity of VIII –VIII, resulted in 10 m height tsunami occurred, 200 died, 2-3 m subsidence in Mapaga village and 2-3m subsidence.

February 2, 1969 earthquake: This earthquake happened at the epicenter of -3.1 S° and 118.5 E° with the magnitude of 6. South Sulawesi, Majene area felt maximum intensities of VIII with thrust fault mechanism, resulted in 2 to 6m height tsunami occurred, 64 killed and over 1,200 buildings were wrecked. Eighty percent of the brick structures were damaged, and some completely collapsed. Ground fissures were noted in several places. Several wooden houses located at the end of a bay were swept away by the waves. The press reported that the tsunami took 600 lives.

March 3, 1977 earthquake: This earthquake occurred at -1.99 N° and 123.05 E° with the magnitude of 5.4 and the depth of 58km.

January 8, 1984 earthquake: This earthquake occurred at -2.77 S° and 118.8 E° with the magnitude of 6.6. The maximum intensity of the earthquake was VII in Mamuju area with thrust fault mechanism.

January 1, 1996 earthquake: This earthquake happened at -0.83 N° and 120.1E° with moderate and high intensities in regional scale with the magnitude of 7.7. It shocked West coast Central Sulawesi area, resulted in 1 to 3.4 tsunami height occurred, 0.5 to 2 m subsidence, 9 killed and 63 injured.

January 23, 2005 earthquake: This earthquake occurred at -1.198 S° and 119.933 E° with the magnitude of 6.3 and the depth of 20 km in Sulawesi.

January 21, 2007 earthquake: This earthquake happened at 1.222 S° and 126.395 E° with the magnitude of 7.5 and the depth of 22 km in Molucca Sea.

November 17, 2008 earthquake: This earthquake originated at -1.29 S° and 122.10 E° with the magnitude of 7.3 and the depth of 30km in Minahasa, Sulawesi.

August 30, 2011 earthquake: This earthquake occurred at 6.401 S° and 126.774 E° with the magnitude of 6.8 and the depth of 465 km.

August 18, 2012 earthquake: This earthquake happened at -1.21 S° and 120.08 E° with the magnitude of 6.2 and the depth of 40km. In Kulawi, Palu City, resulted in heavy damaged buildings.

In Fig. 2, the yellow circle indicates the most affected earthquake potentials can be expected within the radius of 200 km and the red circles indicate distribution of epicenters of the earthquakes based on Digital Elevation Model from SRTM satellite image in 30 meter resolution. The variation in sizes of the circle suggests relative magnitude.

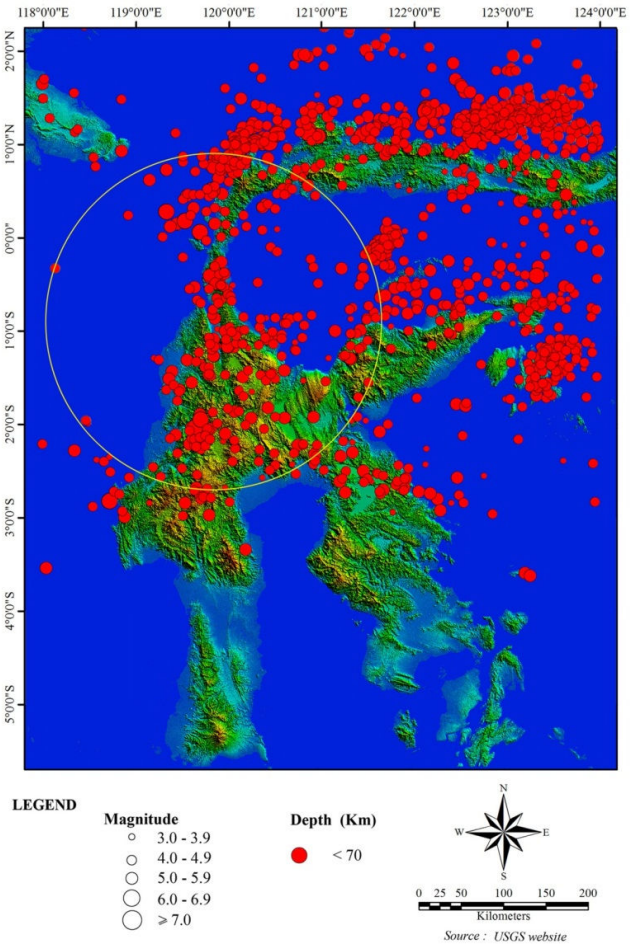

Fig. 2 Epicentral distribution of some important earthquakes around Palu province

III. Digital Elevation Model

Palu depressions are interpreted as a result of pull-apart extension due to sinistral displacement of the fault. This sinistral displacement observed from offset of the rivers along the fault, i.e.: 100-600 m along the Palu-Koro fault [3] and 200 - 600m along the Matano fault. Geometry of Palu depression is up to 7 km wide and bordered by N-S oriented, up to 60 m high steep triangular facets and truncated alluvial fans at West side, and gently step faults at East side, along approximately 20 km length, from Palu bay to the north and Gumbasa valley to the south.

The digital elevation model of the Palu region was applied so as to take the measures needed for the City of Palu located on the segments of the Palu-Koro Fault Zone (PKF), a settlement with earthquake risk on the natural disaster. Geotechnical data and data produced from aerial photos were integrated and assessed on a GIS environment. The topography of the Palu region can be combined topographic map, 1:50000 scale, and digital elevation model (DEM) from SRTM with 30m resolution, to determine structural lineaments (Fig. 3).

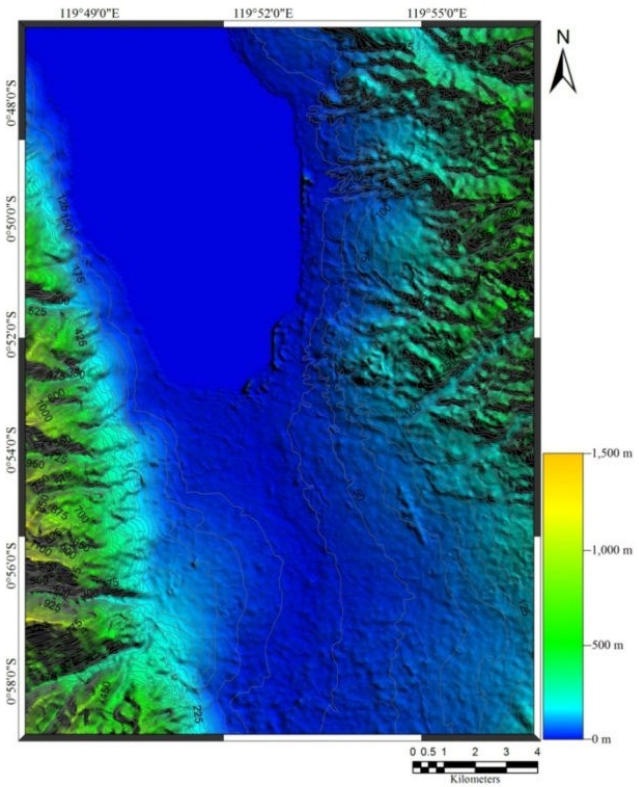

Fig. 3 DEM at Palu area

IV. Geology

Sulawesi, Eastern Indonesia, is a K-shaped island lying at the junction of Eurasia, Indo-Australian and Pacific plates, in a complex region where subduction and collision have been and are still active. Based on the occurrence of distinct rock assemblages, the island can be subdivided into three main geological provinces, namely: (i) West Sulawesi, where Tertiary sediments and magmatic rocks are prominent, (ii) Central and South-East Sulawesi, mainly made up of Early Cretaceous metamorphic rocks and (iii) East Sulawesi, where a huge ophiolitic nappe rests on Mesozoic and Paleozoic sedimentary rocks. The West Sulawesi magmatic province includes the southern arm of Sulawesi, the Western part of Central Sulawesi and finally the Northern arm which extends from Palu to the Manado area [4], [5].

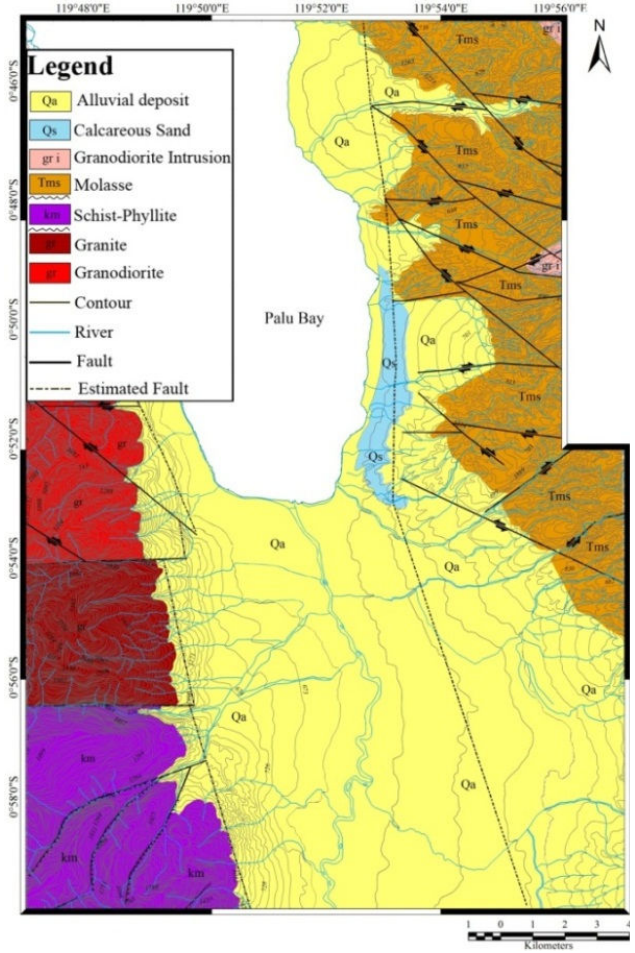

Fig. 4 Geological map of Palu depression area

One of the major structures in Central Sulawesi is the Palu-Koro Fault system, which extends NNW- SSE direction and cross cuts Sulawesi along more than 300 km, from the North Sulawesi trench pass through Palu Bay, southward turn to the SE connect to the Matano and Lawanopo Faults and further eastward, both faults join to Tolo trench [6]. Evolution of Neogene kinematics along the Palu-Koro fault was confirmed based on microtectonics approach, i.e.: sinistral strike-slip due to E-W compression, radial extensions caused by telescoping vertical movement of Neogene granitoid, and then left lateral with normal component displacement due to N-S extension/ E-W compression which is still active actually [7]. Palu depression area is filled by most of clay, silt, and sand deposits as alluvial deposits except on the border east or west consist of gravelly sands as colluvial wedges .The composition of gravel is granitic fragment to the northwest, mostly of schist on the west and to the east the gravel consists of schist, igneous and sedimentary rocks. West escarpment to the north consists of granite and granodiorite units, and to the south consists of schist-phyllitic units. East escarpment consists of molasses [8]. Fig. 4 shows geological map of Palu depression area [9]-[12].

V. Microtremor Survey Instruments

Network sensor model CV-374 AVT instrument was used for the microtremor measurement of 8 points along the array observation lines (Fig. 5). Table I shows adjustment parameters for CV-374 network sensor model.

TABLE I
NETWORK SENSOR MODEL CV-374 AVT

Model	CV-374
Maker	Tokyo Sokushin Co. Ltd.
Developed in	2009
Sensor type	SQ-32 (negative feedback)
A/D converter	24-bit
Sampling frequency	100, 200, 500, 1000 Hz
Amplitude range	±2 G
Frequency range	DC ~ 100 Hz
Trigger level	variable (0.5 ~ 100 cm/s^2)
Pre-trigger time	1 ~ 300 sec.
Post-trigger tim	10 ~ 300 sec.
Number of channels	3
Dimensions and weight	W18 cm x D12 cm x H10 cm, 1.5 kg

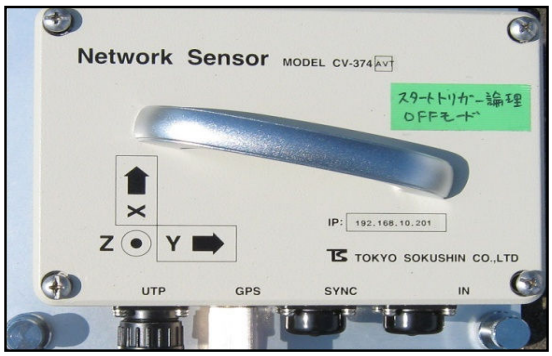

Fig. 5 Instrument of Network Senor Model VC-374 AVT

Microtremor GPL- 6A3P Model, Mitutoyo Corporation was also used for microtremor measurements in Palu City. All instruments have 3 sensors and measures for 3 direction; N-S, E-W and U-D (Fig. 6).

Fig. 6 Instrument of Microtremor GPL- 6A3P Model, Mitutoyo Corporation

VI. Microtremor Single Station Survey

Palu City, a three-component accelerometer with data logger, GPL-6A3P, produced by the Mitsutoyo Co. Ltd., was used for disaster mitigation. Palu City had been applied for evaluation of fundamental frequency and spectral ratio between horizontal and vertical components (H/V Ratio).The number of single microtremor survey was 151 (Fig. 7). The sampling frequencies were 100 Hzor 500 Hz and the observation times were 10 to 15 minutes.

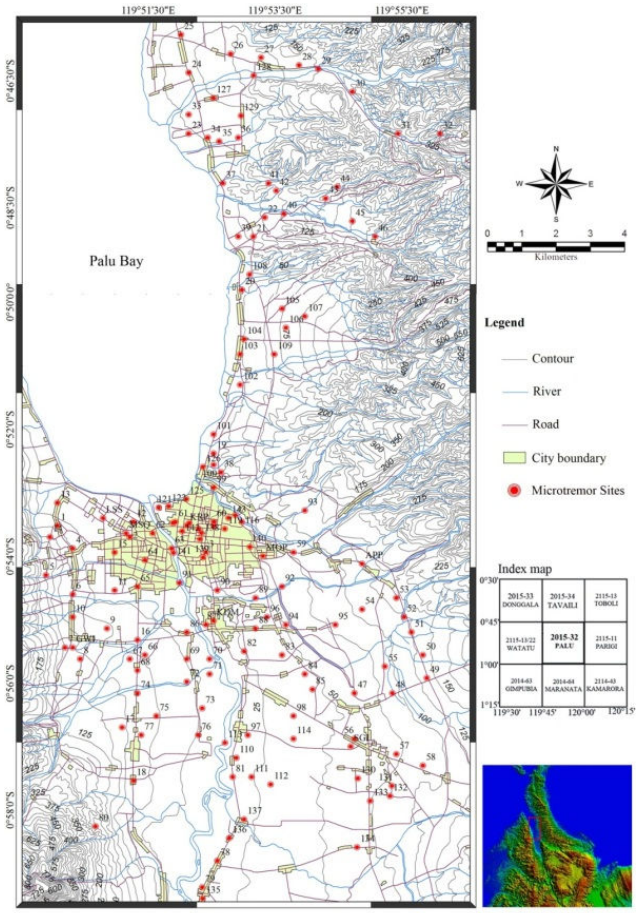

Fig. 7 Location of the microtremor survey sites

The predominant period is defined as the period of vibration corresponding to the maximum value of the Fourier amplitude spectrum. The predominant period is generally obtained from a smoothed spectrum so that undue influence of individual spikes of Fourier amplitude spectrum can be avoided. The spectral ratio of horizontal and vertical motion obtained by microtremor observations is called the H/V spectrum [13]. The predominant period of an H/V spectrum is thought to be equivalent tothe predominant period of the ground directly beneath the site. We identified the H/V spectra calculated into three types according to the shape of the spectra.

Type A: with short period peak (Fig. 8 (a))
Type B: with long period peak (Fig. 8 (b))
Type C: those without clear peaks (Fig. 8 (c))

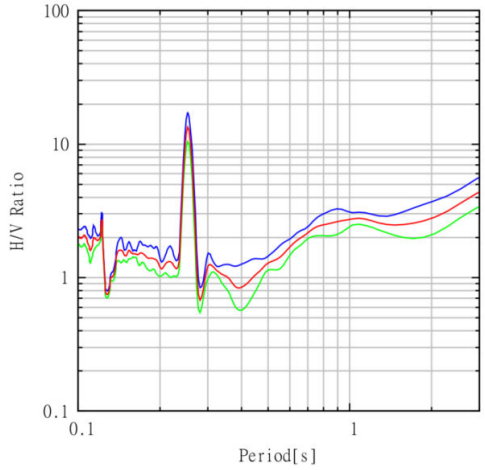

(a) Short period peak

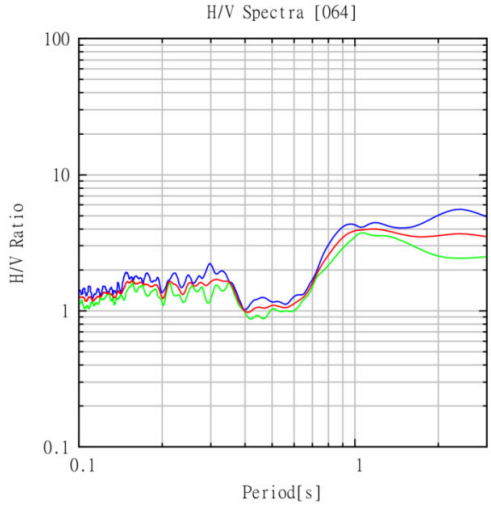

(b) Long period peak

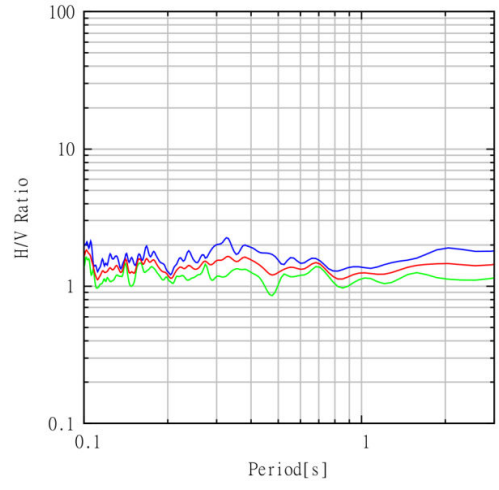

(c) Without clear peak

Fig. 8 Example of the H/V Spectrum ratio (a) short period peak and (b) long period peak (c) without clear peak (mean value and 1σ)

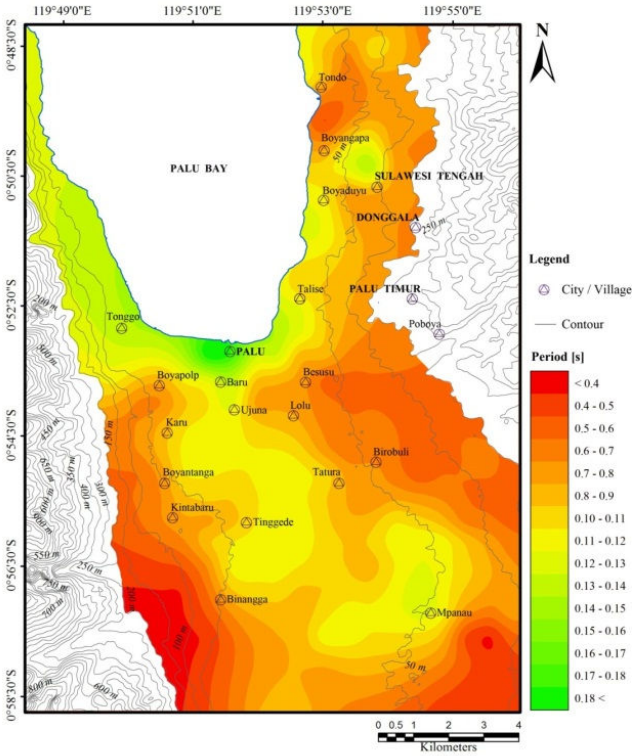

Fig. 9 Spatial distributions map of shorter and longer predominant period

Equation (1) shows the method used to calculate HVSR using the observed records.

$$HVSR = \frac{\sqrt{(F_{NSi}(\omega))^2 + (F_{EWi}(\omega))^2}}{F_{UDi}(\omega)} \quad (1)$$

where, F_{NSi} (ω) and F_{UDi} (ω) denote the Fourier amplitude of the NS, EW and UD components of each interval, respectively, and (ω) is the frequency.

Microtremor single surveys from the distinct peaks express the characteristics of the layers for which the shear wave velocity is quite different. Microtremor survey results of shorter and longer periods are corresponding to a shallow and a deep soil layer. Type A and B reflect an effect of the shallow and the deep soil layer, respectively. Type C is an observation site that has hard soil. Thus, we established the data for both long and short predominant periods. Although there are 151 observation points, the points are not adequate to cover all the target area. If each value of the predominant period obtained is considered to be a realization of a stochastic random field. Space interpolation is conducted by ordinary kriging technique [14]. The results are shown in Fig. 9. According to the results of microtremor survey, Palu City had deposited by fluvial depositional environment. The predominant periods of 1.0- 1.8 seconds were on the alluvial fan area.

VII. Microtremor Array Survey

We carried out array observations at eight sites in Palu City (Fig. 10). Microtremor array survey was conducted by four accelerometers at several districts in Palu City. Four accelerometers were used in each array observation site. One was installed at a center of the circle with a radius, r. Other three were arranged on the circle with a shape of regular triangle. Observation duration time was 20-30 minutes and sampling frequency was 100 Hz. Sequential observations were conducted three times by changing the array radius; r=3, 10 and 30 meters. Then, a substructure profile was identified from the dispersion curve by using the Particle Swarm Optimization [15]-[17].

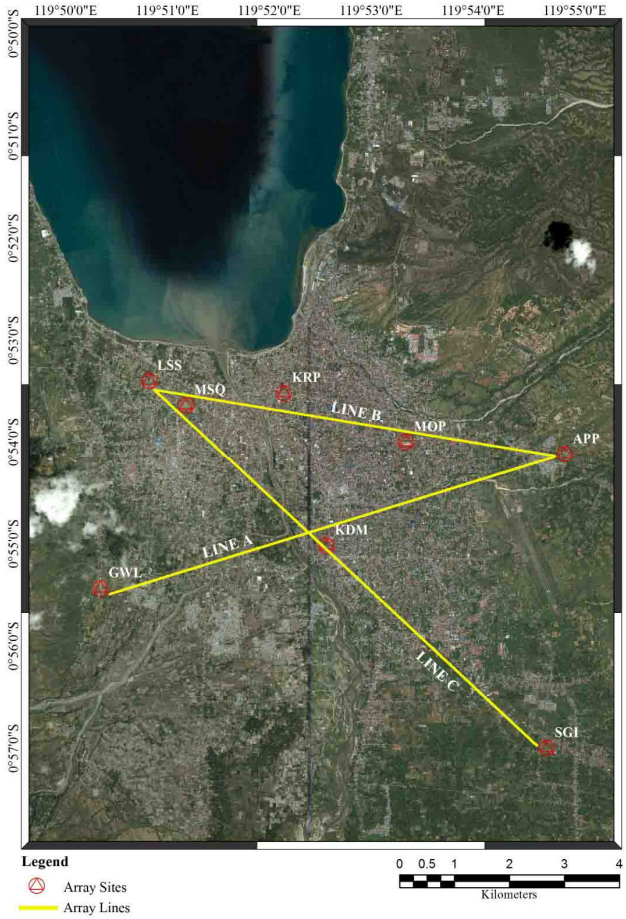

Fig. 10 Three survey lines for array observation (Line A, Line B, and Line C)

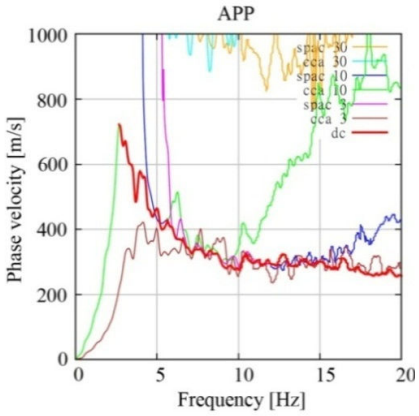

(a) Dispersion curve at APP site

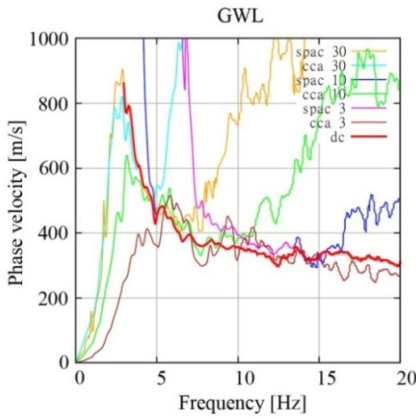

(b) Dispersion curve at GWL site

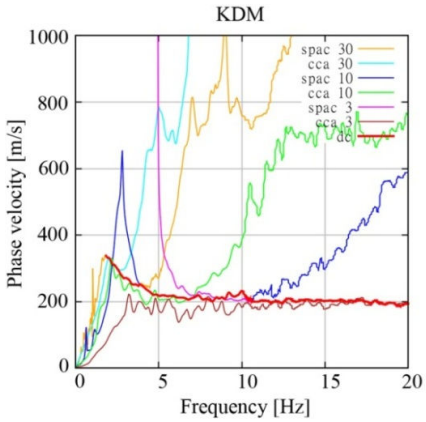

(c) Dispersion curve at KDM site

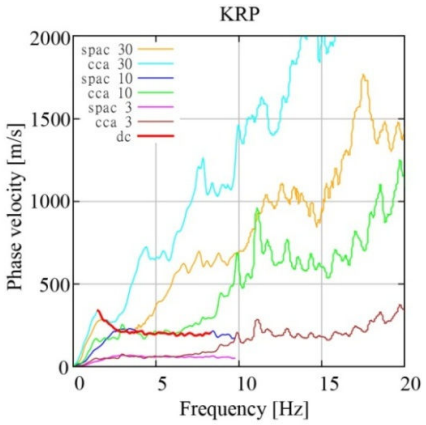

(d) Dispersion curve at KRP site

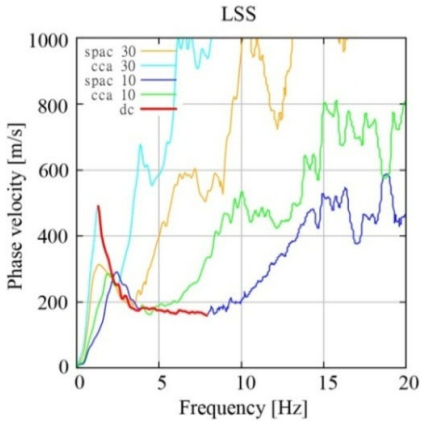

(e) Dispersion curve at LSS site

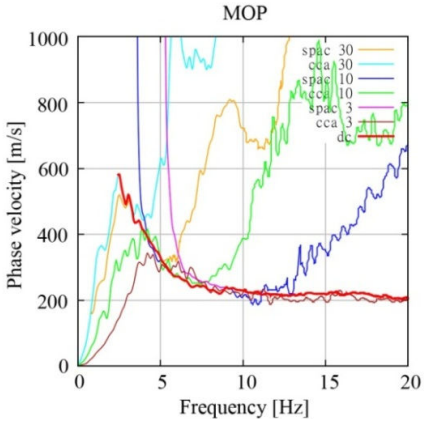

(f) Dispersion curve at MOP site

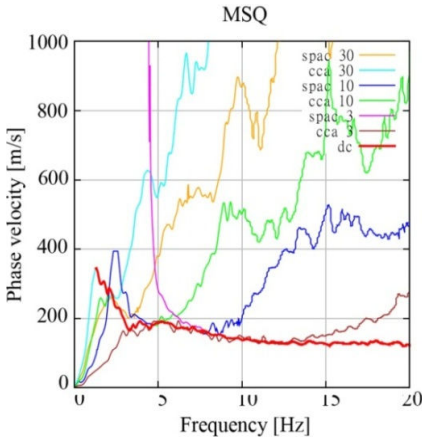

(g) Dispersion curve at MSQ site

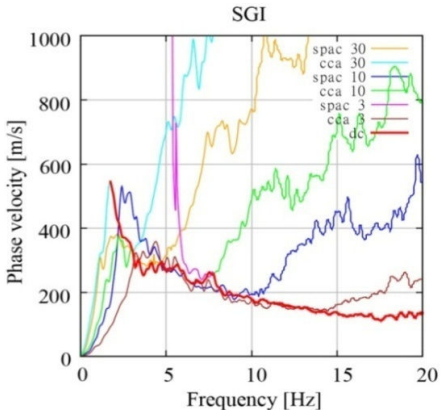

(h) Dispersion curve at SGI site

Fig. 11 Dispersion curves obtained from array survey line (a) APP, (b) GWL, (c) KDM, (d) KRP, (e) LSS, (f)MOP, (g) MSQ and (h) SGI sites

Dispersion curves were calculated using the SPAC and CCA method. The dispersion curves obtained are shown in Fig. 11. Fig. 12 shows Vs structures of the ground along the survey lines (a) Line A, (b) Line B and (c) Line C.

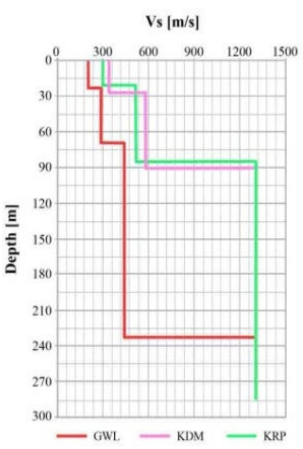

(a) Line A

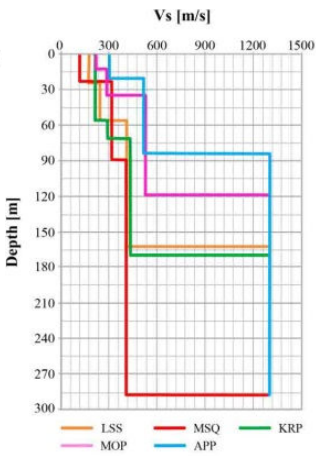

(b) Line B

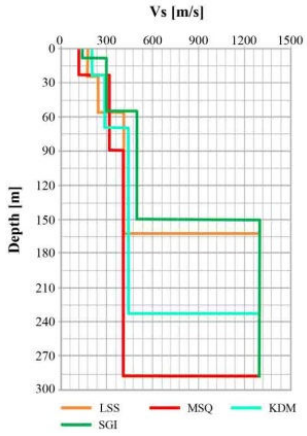

(c) Line C

Fig. 12 Vs structures of the ground along the survey lines (a) Line A, (b) Line B and (c) Line C

For line A, the phase velocity corresponding to shallow ground with a high frequency range is about 369 m/s at APP, about 423 m/s at GWL, about 318 m/s at KDM, about 318 m/s at KRP, about 279 m/s at LSS, about 348 m/s at MOP, about 285 m/s at MSQ and about 317 m/s at SGI. The soft ground extended beneath LSS, which is the nearest site to the coast. The ground beneath the sites higher than GWL has relatively hard surface soil compared with the plain along the coast. Since the minimum phase velocity in the high frequency range is around 300 m/s, the soil profile is very similar along line B and line C. The dispersion curves obtained here had no discrepancies in the distribution of topography, altitude and predominant period. We could estimate subsurface sedimentary layers in the plains using these dispersion curves

VIII. Site Classification

The site classification is provided according to SNI-1726-2002, in which soil condition is classified into three types: (1) soft soil, (2) medium dense soil, and (3) hard or dense soil based on final S-wave velocity structures shown in Table II, Vs is determined by using the regular triangle shape circular array.

TABLE II
Site Classification at Palu City by SNI-1726-2002

No	Area	V_s(m/s)	Weak soil Vs<175(m/s)	Medium Dense Soil $175 \le V_s \le 350$ (m^{-s})	Dense Soil $V_s \ge 350$ (m^{-s})
1	APP	369.7			✓
2	GWL	423.7			✓
3	KDM	318.1		✓	
4	KRP	318.0		✓	
5	LSS	279.0		✓	
6	MOP	348.0		✓	
7	MSQ	285.7		✓	
8	SGI	317.8		✓	

As shown in Table II, the average S-wave velocity of the depth Vs, at all eight sites is between 279.0 and 423.7 m/s. Except from APP and GWL sites, all sites are belong to medium dense soil. APP and GWL sites are belongs to dense soil. The S-wave velocity structures of Central Sulawesi province, especially in Palu City had been successfully evaluated and these are one of the main inputs for 1D Equivalent Linear Seismic Response Analysis. For the theoretical simulation of strong ground motion, it is importance to get information of underground structures, especially for sedimentary layers overlying on bedrock, like in Palu City. Shear wave velocity structure is one of the most important parameter for seismic response analysis. The thickness of sediments or depth of bedrock was determined together with S-wave velocity structures. In this process, there are two variables; S-wave velocity and thickness of each sediment layer. The mean velocity structure with normalized depth is regarded to represent the whole studied area and is used for other sites by changing normalized depth to actual depth which can give proper equivalent H/V ratio.

IX. Modeling of Subsurface Structure by Inversion

According to the inversion analysis, the peak of the H/V spectrum at Palu City APP, GWL, KDM, KRP, LSS, MOP, MSQ and SGI, could be explained by the theoretical ground model. The identified soil parameters by the inversion at KRP are shown in Table III. Fig. 13 shows dispersion curve of the ground along the survey lines at KRP.

TABLE III
Identified Ground Parameters at KRP

Layer	P[t/m3]	Vp[m/s]	Vs[m/s]	H[m]
1	1.7	1,069	219	54
2	1.8	1,250	295	15
3	1.9	1,546	439	98

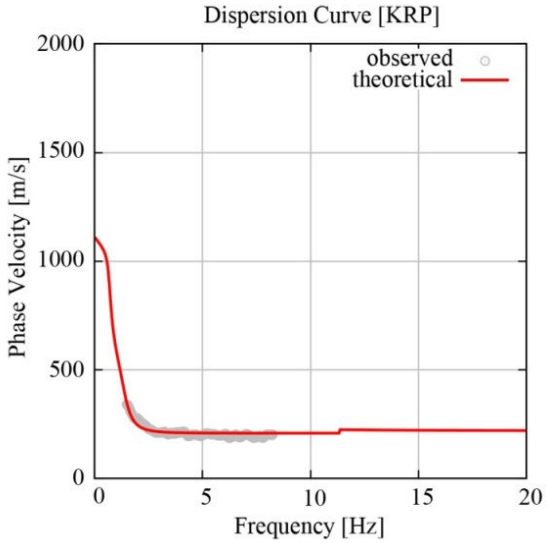

Fig. 13 Dispersion curve at KRP

X. Modeling of Subsurface Structure in Palu City

The peaks in the short and long periods of the observed H/V spectrum could be explained by the estimated subsurface soil structure. In this study, we used the two distinct peaks in the observed H/V spectra and Vs structure obtained by array observation. The technique used was the 1/4 wavelength principle, which can approximately be extended to multilayered media.

$$H = \frac{1}{4} \cdot V_s \cdot T \tag{2}$$

where, H is a thickness of a layer. Here we divided the ground into three layers; the upper two layers and a base semi-infinite layer. The range of the shear wave velocity for the first, second and third layers is assumed (I) $Vs \leq 300$ m/s, (II) $300 \leq Vs \geq 13000$ m/s and (III) $Vs \geq 13000$ m/s. Fig. 14 shows three dimensional shape of the estimated subsurface soil structure. The distribution of thickness for the first layer of which $Vs$is $\leq$ 300m/sec in Palu area is shown in Fig. 15, in which the rapidly varying area of the subsurface condition and dense observation area are enclosed.

The ground model is constructed as follows: The rectangular area (about 28 km ×10 km) and it was divided into 1×1 meshes (1km square). According to the Kriging technique, the values of predominant periods, Ts, at the center of each mesh are interpolated by using the finite number of peak periods read from the observed H/V spectrum.

The shear wave velocities, Vs, of layer-I and layer-II are calculated by the weighted average, for which the weight is the reciprocal of square of distance from the array observation points, APP, GWL, KDM, LSS, MOP, MSQ and SGI, as

$$\overline{V_s} = \frac{\sum \frac{V_{Si}}{x_i^2}}{\sum \frac{1}{x_i^2}} \tag{3}$$

where i defines the array site ($i=1,2,...,7$), and xi indicates the distance between an array observation site and the center of the mesh.

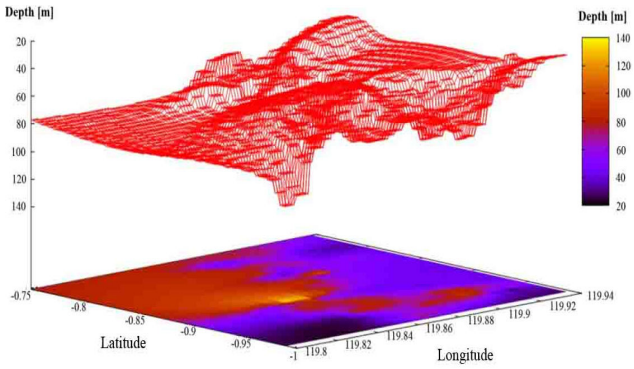

Fig. 14 Three dimensional shape of the estimated subsurface soil structure

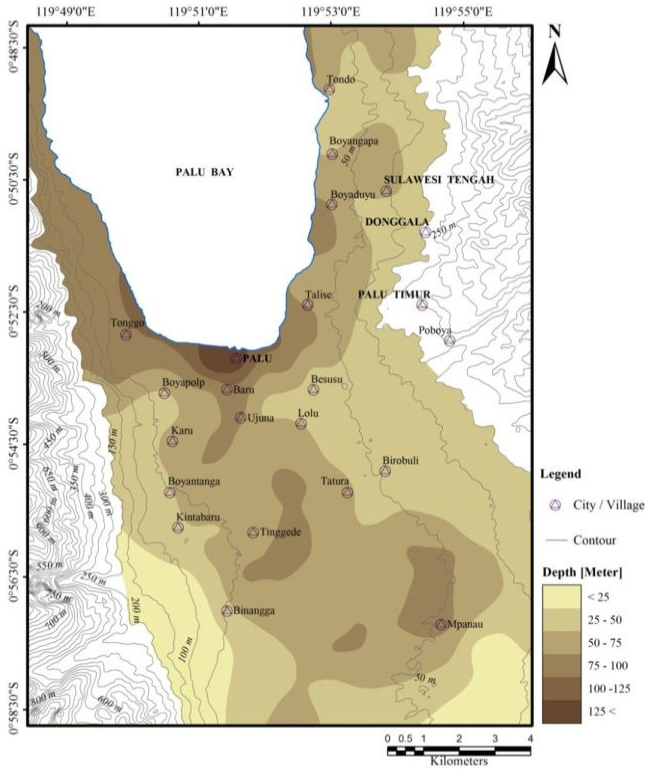

Fig. 15 Depth of the engineering bed rock or sediment thickness

XI. Strong Ground Motion by Empirical Stochastic Green's Function

The strong ground motion in Palu City were predicted based on the empirical stochastic Green's function method and it was used by the synthetic waveforms of 2005 Palu earthquake as input bedrock motion below the alluvium sediments. The Irikura's computer code [18], [19] was used to generate synthetic waveforms, mainly based on epicentral distance, magnitude and focal depth of earthquake. In this research, ground model for Palu City is constructed by combining two layer model and average seismic bed rock model used in Japan, because there is no bed rock information in this area. The Palu-Koro Fault model referred is an earthquake with moment magnitude of 6.3 on 23 January 2005 in Palu, Indonesia, of which epicenter was latitude 119.933 and longitude -1.198. Fig. 16 shows the location of the Palu-Koro fault and epicenter.

XII. Peak Ground Acceleration Due to Strong Ground Motion

Peak Ground Acceleration, PGA, is commonly used to describe ground motion because of their natural relationship to inertial force induced in certain types of structures are closely related to it. Based on acceleration histories of response analysis, PGA values are determined. During dynamic response analysis, PGA had been determined based on response acceleration spectrum and acceleration time histories

of array sites. The PGA value is generally ranging from 100 gals to 550 gals.

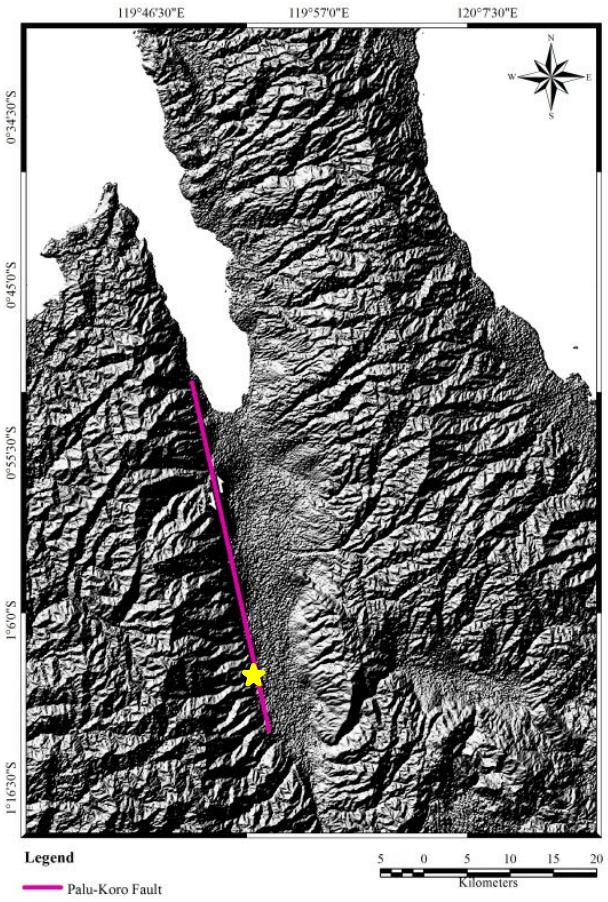

Fig. 16 The location of the Palu-Koro fault and epicenter

The central portion, high damage area, especially around Binangga of Palu show high PGA value, 400-500 gals. Around Boyantanga, Kintabaru and Tinggede area shows 300 -450 gals. The PGA at Boyapolo and Tonggo are 350-450 gals while PGA is less than 350 gals in Palu and Talise areas. The component of the shaking is NS direction. There are high accelerations and velocities are as appears along the fault, especially near the epicenter. There occurred relatively large shaking at the mouth of Palu river because of the deeper thickness of the sediment. The PGA map of Palu area is shown in Fig. 17.

XIII. Peak Ground Velocity due to Strong Ground Motion

The peak ground velocity, PGV had been determined during response analysis as an output of time-history for first 15 s for all 151 sites in studied area. PGV is one of the main parameter for estimation and prediction of damage intensity and epicentral area. Peak velocity is a useful parameter for characterization of ground motion amplitude. At Binangga and Boyantanga sites, peak velocity was observed at high velocity. The PGV map of Palu area is shown in Fig. 18.

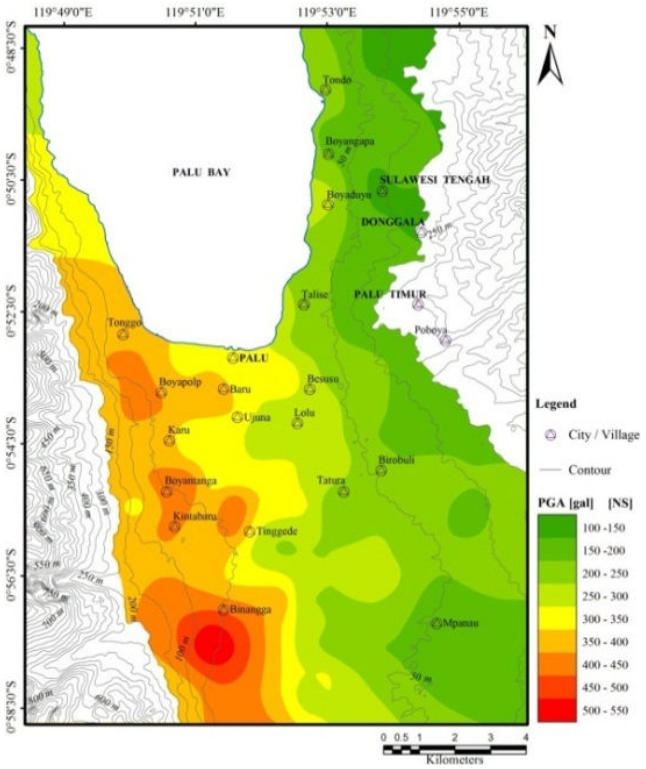

Fig. 17 Peak ground acceleration [NS] map on Palu area

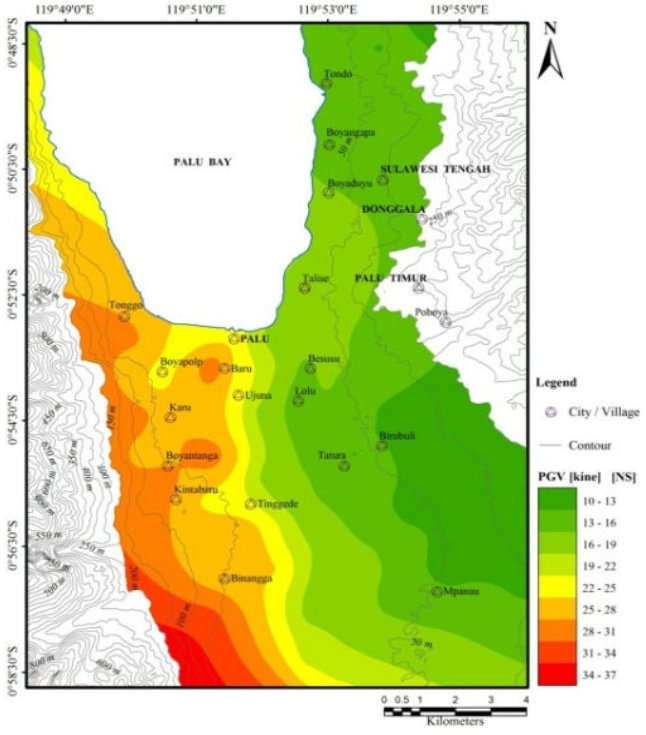

Fig. 18 Peak ground velocity [NS] map on Palu area

XIV. Seismic Vulnerability Index Due to Strong Ground Motion

Seismic vulnerability index $K_g$value is calculated and verified to estimate the validity by comparing it with the past earthquake of 2005. Seismic vulnerability index is obtained by squaring the HVSR spectrum with a peak value of the frequency and is defined [20] as:

$$K_g = \frac{A^2}{f_0} \tag{4}$$

with K_g the seismic vulnerability A index is HVSR spectral peaks and f_0 the resonance frequency.Seismic vulnerability index is also related to geomorphological and geological conditions showed that the high seismic vulnerability indicated that in Palu bay areas were composed by alluvial material and calcareous deposits. Seismic vulnerability index in Palu City found that the high seismic vulnerability indicated scattered in the alluvial and coastal deposits area. In the hill area, seismic vulnerability index shows a very low value. The survey results showed that in hilly areas had low seismic vulnerability index, whereas in coastal alluvium was composed of material having a high seismic vulnerability indication (Fig. 19).

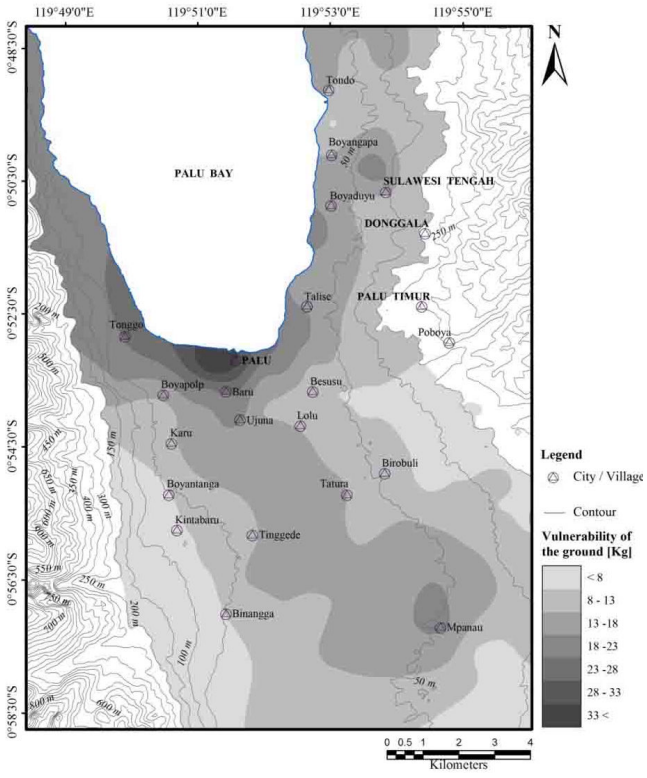

Fig. 19 Map of seismic vulnerability index in Palu City

XV. Ground Shear Strain Due to Strong Ground Motion

Earthquake disaster is caused by the earthquake static load and the vulnerability of ground and structures, which receive it. Earthquake load includes static load such as fault movement and dynamic load by earthquake motions. The vulnerability index is expected to be generalized as compared with actual earthquake damage. When shear deformation at ground surface at the time of earthquake is set to δ_g, the strain of surface ground $\gamma_g$is expressed as follows in approximation:

$$\gamma_g = \delta_g / h \tag{5}$$

$$= \mathrm{e} \times \mathrm{a} / (2\pi F_g)^2 \times 4F_g / V_s$$

$$= \mathrm{e} \times Ag \times \mathrm{a} / (\pi^2 F_g V_b)^2 \times V_b / V_s$$

$$= \frac{Ag^2}{F_g} \times \frac{e \times a}{\pi^2 \times V_b}$$

$$= K_g \times \mathrm{C} \times \mathrm{a} \tag{6}$$

$$K_g = A_g^2 / F_g \tag{7}$$
$$\mathrm{C} = e/(^2.V_b)$$

where,

γ_g:Shear strain (in powers of 10^{-6})

Ag: Amplification factor of the surface ground $= V_b / V_s$

F_g: Naturalfrequency of the surface ground (Hz) $= V_s/4h$

a : Maximum acceleration of the basement (Gal)

e : Efficiency of the maximum acceleration

V_b: S-wave velocity of the basement (m/s)

V_s: S wave velocity of surface ground (m/s)

h: thickness of surface ground

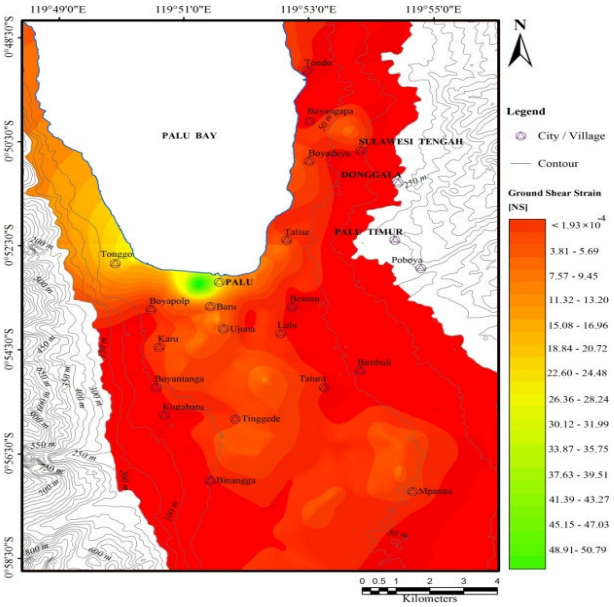

Fig. 20 Map of ground shear strain (NS) in Palu City

Here, if it is assumed that it is $V_b \leq 1300$ m/s and $e = 0.6$, it is come to $C \fallingdotseq 1.0$. Effective strain can be presumed as a value which multiplied by K_g value and the maximum acceleration in case of an earthquake. K_g value is an index peculiar to the measured ground, and it is possible to express the vulnerability of the ground. As shown in equation (7), K_g value can be easily derived from natural frequency F_g and amplification factor Ag which were presumed in each measurement point. The survey results showed that in hilly areas had low ground shear strain, whereas in coastal alluvium was composed of material having a high ground shear strain indication (Fig. 20).

XVI. Conclusion

The conclusions obtained in this study are as follows.

Subsurface engineering bed rock in Palu City had been successfully determined based on data from array microtremors measurements.

Microtremor observations were carried out for constructing a subsurface ground model in Palu City. Single-point observations and array observations were conducted at 151 and 8 sites respectively, which covered almost the whole city area.

Three dimensional universal Kriging methods can be used for the interpolation of subsurface information such as shear wave velocity and depth of irregular boundary.

We constructed a four layered model in each array observation point. We reconstructed unified two-layered model by averaging the first three layers obtained from array observation.

The shear wave velocity of the top layer is $Vs \leq 300$ m/s. By combining above two-layer model and the results of single point observation, we proposed the distribution of the first layer thickness of the sediment.

The average S-wave velocity of the depth Vs, at all eight sites is between 279.0m/s and 423.7 m/s. Except from APP and GWL sites, all sites are belong to medium dense soil. APP and GWL sites are belongs to dense soil. Strong ground motions of were predicted based on the stochastic Green's function method by using the proposed ground model. Peak acceleration becomes more than 400 gal and peak velocity becomes more than 30 kine, which causes severe damage for buildings in high probability at Palu City.

Microtremor survey results showed that in hilly areas had low seismic vulnerability index and ground shear strain, whereas in coastal alluvium was composed of material having a high seismic vulnerability and ground shears train indication. Palu City had deposited by fluvial depositional environment.

Acknowledgment

This research was supported by the Grant-in-Aid of JICA/AUN SEED-Net. We gratefully acknowledge Dr. Noguchi, Dr. Ono in Tottori University, and Dr. Rusnardi Rahmat Putra in Kyoto University for their cooperation with the microtremor observations. We sincerely thank Gadjah Mada University and Tadulako University for their help in undertaking the observations in Palu, Indonesia.

References

[1] Topographic map of Indonesia, *Sheet no. 2015-32, Palu, 1991 edition*, the coordination of national survey and mapping (Bakosurtanal) Jl.Raya Jakarta-Bogor km 46, biec international, inc bandung, 40116, Indonesia, geodetic construction survey ltd. Zug Switzerland and Swissair photo surveys ltd, Zuerich Switzerland, 1991.

[2] USGS. Historical Worldwide Earthquakes, 2007.

[3] H. D. Tjia, and T. Zakaria. Palu-Koro strike-slip fault zone, Central Sulawesi, Indonesia.Sains Malaysia, 1974, 3 (1), 65-86.

[4] W. Hamilton. *Tectonics of the Indonesian Region, U.S. Geol.Surv. Prof. Paper 1078,* 1979, 345 pp.

[5] R. Sukamto, *Reconnaissance geological map of Palu area, Sulawesi. Geological map, scale 1:250.000*. Geological Survey of Indonesia, Bandaung, Indonesia, 1973.

[6] B. Priadi. Geochimie du magmatisme de l'Ouestet du Nord de Sulawesi, Indonesia: Tracage des sources et implications geodynamique. *Doctoral thesis, Universite Paul Sabatier, Toulouse, France*, 1993.

[7] S. Pramumijoyo,S. Indarto, C. Widiwijayanti, and J. Sopaheluwakan. Seismic Parameters of the Palu-Koro Fault in Palu Depression Area, Central Sulawesi. Indonesia, *J. SE Asian Earth Sci*, 1997.

[8] R.A.B. Soekamto. Regional Geological Map of Palu Sheet, Indonesia, *Scale 1:250,000, Geological Research Center, Bandung*, 1995.

[9] S. R. Ananda. Analisisdan Interpretasi Kelurusan Struktur Geologi Menggunakan Digital Elevation Model (DEM) ASTER Daerah Kecamatan PaluTimurdanSigibiromaru, KabupatenDonggala, Kota Palu, GadjahMada University,2013.

[10] G.I. Aryawan. Analysis danInterpretasiStrukturGeologiMenggunakan Digital Elevation Model (DEM) ASTER Daerah KecamatanMarawola, Dolo, danPalu Barat, Kota Palu, Sulawesi Tengah, GadjahMada University, 2013.

[11] G.F. Ismawan, G. F. GeologidanAnalisisStrukturGeologiBerdasarkan Digital Elevation Model (DEM) ASTER Daerah Palu Barat dan Marawola, Kota Palu, Poopinsi Sulawesi Tengah, GadjahMada University, 2013.

[12] D. Juwanto. Studi Struktur Geologi Tepi Timur Lembah Palu Kecamatan Palu Timut, danTavaili, Kota Palu, GadjahMada University, 2013.

[13] K. Aki. Space and time spectra of stationary stochastic waves, with special referent to microtremor*, Bull. Earth. Res.Inst., Vol.35, No.3*. 1957, pp. 415-456.

[14] J. Kiyono and M. Suzuki. Conditional Simulation of Stochastic Waves by Using Kalman Filter and Kriging Techniques, *Proc. of the 11th World Conference on Earthquake Engineering, Acapulco, Mexico*, 1996, Paper No.1620.

[15] P. S. Thein, S. Pramumijoyo, K. S. Brotopuspito, W. Wilopo, J. Kiyono and A. Setianto. Investigation of Subsurface Soil Structure by Microtremor Observation at Palu, Indonesia, *The 6th ASEAN Civil Engineering Conference (ACEC) & ASEAN Environmental Engineering Conference (AEEC), Civil and Environmental Engineering for ASEAN Community*, Bangok, Thailand. 2013, p. C-6.

[16] T. Noguchi, T.Horio, M. Kubo, Y. Ono, J. Kiyono, T. Ikeda and P. R Rusnardi. Estimation of Subsurface Structure in Padang, Indonesia by Using Microtremor Observation, *Report on Earthquake Disaster Prevention Field, Tono Research Institute of Earthquake Science*, Seq. No.26, 2009, pp. 1-16, (in Japanese).

[17] J. Keneddy and R. C. Eberhart.Particle swarm optimization, Proc. of IEEE International conference on Neural Networks. 1995,Vol.4, pp.1942-1948.

[18] K.Irikura, and H. Miyake. Prediction of strong ground motions for scenario earthquakes. 2001, Journal of Geography 110, 849–875

[19] K.Irikura.,H.Miyake., T.Iwata., K. Kamae., H. Kawabe and L.A Dalguer. Recipe for predicting strong ground motion from future large earthquake, Proceedings of the 13th World Conference on Earthquake Engineering No. 1371, 2004.

[20] Y. Nakamura. Clear Identification of Fundamental Idea of Nakamura's Technique and Its Application*. World Conference of Earthquake Engineering,* 2000.